

Proteomic profiling of biomarkers by MALDI-TOF mass spectrometry for the diagnosis of tracheobronchial stenosis after tracheobronchial tuberculosis

BIHAO PENG¹, XIAOJIAN QIU², ZHIWU DONG³, JIE ZHANG², YINGHUA PEI² and TING WANG²

¹The Second Clinical Medical College, Nanchang University, Nanchang, Jiangxi 330000;

²Department of Pulmonary Diseases, Beijing Tian Tan Hospital, Capital Medical University, Beijing 100050;

³Department of Laboratory Medicine, Shanghai Sixth People's Hospital Jinshan Branch, Shanghai 201599, P.R. China

Received September 29, 2019; Accepted July 14, 2020

DOI: 10.3892/etm.2020.9495

Abstract. Tracheobronchial tuberculosis (TB) leads to airway stenosis, irreversible airway damage and even death. The present study aimed to identify biomarkers for the diagnosis of tracheobronchial stenosis (TBS) secondary to tracheobronchial TB. A cohort was recruited, including patients with TBS after tracheobronchial TB, TBS after tracheal intubation or tracheotomy (TIT) and no stenosis of early-stage lung cancer. Proteomic profiling was performed to gain insight into the mechanisms of the pathological processes. Differentially expressed proteins in the serum and bronchial alveolar lavage fluid (BALF) from patients were detected by matrix-assisted laser desorption ionization time-of-flight mass spectrometry (MALDI-TOF MS). Subsequently, ELISA was performed to validate the changes of protein levels in an additional cohort. MALDI-TOF MS revealed that 8 peptides in the serum, including myeloid-associated differentiation marker, keratin type I cytoskeletal 18, fibrinogen α -chain, angiotensinogen (AGT), apolipoprotein A-I (APOAI), clusterin and two uncharacterized peptides, and nine peptides in BALF, including argininosuccinate lyase, APOAI, AGT and five uncharacterized peptides, were differentially expressed (molecular-weight range, 1,000-10,000 Da) in the TB group compared with the

TIT group. The ELISA results indicated that the changes in the protein levels had a similar trend as those identified by proteomic profiling. In conclusion, the present study identified proteins that may serve as potential biomarkers and provide novel insight into the molecular mechanisms underlying TBS after tracheobronchial TB.

Introduction

Benign airway stenosis may be congenital or acquired, and the causes of acquired airway stenosis include trauma, surgery, tracheobronchial TB, tracheal intubation, tracheotomy, stent insertion and inhalation injury. Airway injury results in edema and erythema of the mucosal layer, which persists as long as the pathogenic factors are present. As a consequence, the ring cartilage is exposed and inflamed, collagen and scar tissue are produced and the ring contracts, resulting in the formation of a hard stenosis covered with epithelial cells (1). Tracheobronchial TB refers to *Mycobacterium tuberculosis* infection of the mucosa, submucosa, smooth muscle, cartilage and the outer membrane of trachea and bronchus (2). With an increasingly mobile population and the continuing human immunodeficiency virus acquired immunodeficiency syndrome pandemic, the numbers of patients with TB are gradually increasing and the incidence of tracheobronchial TB in patients with active TB ranged from 6.4 to 40% in Iran, 2014 (3). Of all patients with tracheobronchial TB in India (2014), >90% suffered from airway stenosis to varying degrees (4). A previous study demonstrated that an age of >45 years, fibrostenotic subtype and anti-TB chemotherapy are independent clinical predictors of persistent airway stenosis (5). However, only a small number of clinical biomarkers have been identified for the diagnosis of tracheobronchial stenosis (TBS) after tracheobronchial TB. Currently, TBS is confirmed by clinical manifestations, chest CT (6) and bronchoscopy (7); however, there is a lack of rapid and effective laboratory indicators. As it is difficult to differentiate TBS after TB from other lung diseases, including TBS after tracheal intubation or tracheotomy (TIT), the condition is frequently diagnosed at a late stage and numerous patients have missed the optimal time window for treatment (8). With early diagnosis, clinicians are able to provide appropriate and

Correspondence to: Dr Jie Zhang, Department of Pulmonary Diseases, Beijing Tian Tan Hospital, Capital Medical University, 6 Tiantanxili Street, Beijing 100050, P.R. China
E-mail: zhangjiettyhxxk@163.com

Abbreviations: TBS, tracheobronchial stenosis; TB, tuberculosis; TIT, tracheal intubation and tracheotomy; ESLC, early-stage lung cancer; BALF, bronchial alveolar lavage fluid; MS, mass spectrometry; MALDI, matrix-assisted laser desorption/ionization; TOF, time-of-flight; MB-WCX, weak cation exchange magnetic beads; MYADM, myeloid-associated differentiation marker; FGA, fibrinogen α -chain; AGT, angiotensinogen; CLU, clusterin

Key words: tracheobronchial stenosis, tuberculosis, proteomics, biomarker, bronchial alveolar lavage fluid

timely therapy, preventing the development of airway stenosis and improving the patients' prognosis (9).

Proteomics generally refers to large-scale studies of all of the proteins in cells, tissues or organisms, or in specialized samples, including body fluids (10). Proteomics consists of overall protein profiling, including expression levels, structure, interactions and modifications after translation; therefore, it represents a noninvasive method to diagnose various diseases (11). In the last few decades, proteomics has provided extensive data and insight into the pathophysiological mechanisms of numerous human diseases, including carcinoma, infection and coronary heart disease, as well as the identification of novel biomarkers and therapeutic targets for clinical diagnostics and treatments (12). Proteomics primarily involves two-dimensional gel electrophoresis, western blotting, immunoprecipitation and mass spectrometry (MS) (13).

MS is used to identify chemical compounds by ionizing them into charged molecules and separating the ions by their mass-to-charge ratio (m/z) (14). Since the introduction of the application of matrix-assisted laser desorption/ionization (MALDI) in the 1990s, MS has been widely used to profile large biological molecules (15). Large biological molecules, including DNA, proteins and sugars, are ionized by gaining or losing a proton without affecting the characteristics of the sample. The sample to be detected is dispersed into matrix material located on a metal plate and the sample and the matrix are irradiated by a pulsed laser and vaporized. The target molecules are then ionized and ready for acceleration by MS. Time-of-flight (TOF) MS examines the time it takes for ions to cover fixed distances with velocities determined by their m/z (16). In theory, ions with small m/z values or with more charges will reach the detector earlier; thus, an m/z value is determined by the time of flight and the molecule is identified accordingly. Considering MALDI-TOF MS has high-throughput capability and can be completely automated, it is ideal for proteomics research (17,18).

Proteomic changes in airway stenosis evoked by tracheo-bronchial TB have remained largely undefined. The aim of the present study was to compare protein expression profiles in the sera and bronchoalveolar lavage fluids (BALFs) to clarify the pathogenesis of TBS after tracheobronchial TB.

Patients and methods

Patients. A total of 91 patients with TBS after TB, TBS after TIT and early-stage lung cancer (ESLC) were enrolled at the Department of Respiratory Diseases, Beijing Tian Tan Hospital, Capital Medical University (Beijing, China) from January 2014 to October 2018. Patients enrolled between January 2014 to October 2015 were subjected to MS analysis and patients enrolled between November 2015 to October 2018 to ELISA. Patients with TBS after TB, TBS after TIT and ESLC had been confirmed by chest CT scan and clinical testing, including reverse-transcription PCR assay for TB and tumor markers of CEA, CA15-3, CA19-9, CA125, neuron-specific enolase and cytokeratin fraction 21-1. All of the patients provided written informed consent to participate in the present study and for use of their medical data according to the provisions of the Declaration of Helsinki. The protocol of the present study was approved by the Institutional Ethics Committee of Beijing Tian

Tan Hospital. The serum and BALF samples from 31 patients were subjected to MALDI-TOF MS and their characteristics are presented in Table SI. The serum samples from the other 60 patients (20 with TB, 20 with TIT and 20 with ESLC) were used for validation with ELISAs (Table SII). There were no significant differences in age and sex between groups.

Sample collection. Serum samples were collected, processed and stored in according to a technique similar to a standard protocol (19). Blood samples were obtained from fasted patients in the morning (collected in vacuum tubes without preservatives or anticoagulant) and allowed to clot or to sediment at room temperature ($\sim 25^{\circ}\text{C}$) for 2 h to isolate the serum. Serum samples were then separated by centrifugation at $3,000 \times g$ at 23°C for 15 min. Samples were immediately divided into aliquots of $50 \mu\text{l}$ and stored at -80°C until further analysis. The cryopreservation period for serum samples was <24 months.

BALF samples were collected and processed according to a standard protocol (19). Samples were separated by centrifugation at $4,000 \times g$ for 15 min at 4°C . Supernatants were aliquoted into four 1 ml tubes and the precipitate was added into one 1ml tube. The samples were stored at -80°C until use. The cryopreservation period for BALF samples was <24 months.

Weak cation exchange magnetic bead (MB-WCX) fractionation and MALDI-TOF MS analysis. All of the samples were fractionated using MB-WCX (Bruker Corporation), according to the manufacturer's protocol. The suspension was prepared with a magnetic bead-weak cation exchange MB-WCX kit (Bruker Corporation) and mixed by shaking. Following eluting and shocking, the magnetic beads were separated from the protein and the eluted peptide samples were transferred to a clean 0.5 ml tube for further MS analysis. A total of $5 \mu\text{l}$ of hydroxy-cyanocinnamic acid substrate solution (0.4 g/l; MilliporeSigma; dissolved in acetone and ethanol) and 0.8-1.2 μl of eluate were mixed. Subsequently, 0.8-1.2 μl of the mixture was applied to a metal target plate and dried at room temperature. Finally, air-dried target plates were measured immediately using a calibrated Autoflex III MALDI-TOF MS (Bruker Corporation) with Flex-Control software (version 3.0; Bruker Corporation), according to optimized measuring protocols (20). Peptides with molecular weights ranging from 1,000 to 10,000 kDa were collected with a laser intensity of $5,000 \text{ W/nm}^2$. Peptide mass fingerprints were obtained by combining 50 individual MS signal scans. ClinProTools software (version 2.2; Bruker Corporation) was used to subtract the baseline, normalize spectra (using the total ion current) and determine peak m/z values and intensities in the mass range of 1,000-10,000 kDa. A signal-to-noise (S/N) ratio of >5 was selected to guarantee for clear acquisitions. An S/N of >3 was used for limit of detection and an S/N of >5 was used for quantification. Spectra were aligned with a mass shift of $\leq 0.1\%$. The peak area was measured for quantification. Based on the macroscopic results of the multivariate statistical analysis, the tendency of the relative integrals of each metabolite to change in the three groups was further analyzed by box-and-whisker plots.

ELISA. ELISA was performed to confirm the changes in the levels of myeloid-associated differentiation marker

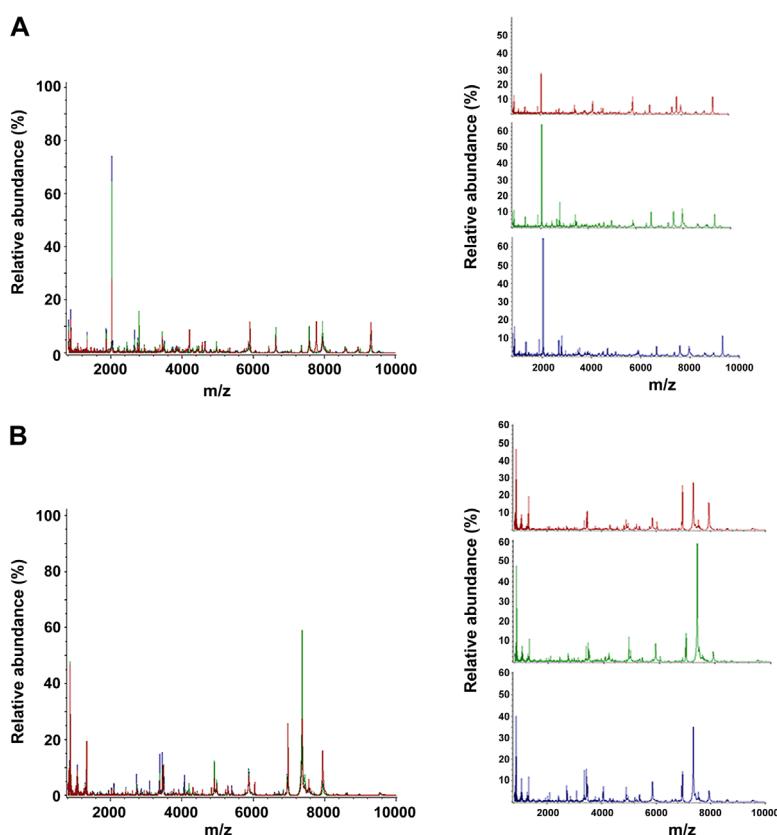


Figure 1. Comparisons of peptide profiles in serum and BALF. (A) Serum spectra in the mass range of 1,000-10,000 kDa obtained from TB patients (red), TIT patients (green) and ESLC patients (blue). (B) BALF spectra in the mass range of 1,000-10,000 kDa obtained from TB patients (red), TIT patients (green) and ESLC patients (blue). BALF, bronchial alveolar lavage fluid; m/z, mass-to-charge ratio; TBS, tracheobronchial stenosis; TB, tuberculosis; ESLC, early-stage lung cancer; TIT, tracheal intubation and tracheotomy.

(MYADM), keratin, type I cytoskeletal 18 (KRT18), fibrinogen α -chain (FGA), angiotensinogen (AGT), apolipoprotein A-I (APOAI) and clusterin (CLU) in serum from another cohort of patients who were not subjected to MS analysis. This cohort included 20 patients with TB, 20 with TIT and 20 with ESLC. KRT18 (cat. no. MA1-19041; 1:5,000), FGA (cat. no. MA1-20038; 1:5,000), AGT (cat. no. MA5-29009; 1:10,000) and APOAI (cat. no. MIA1402; 1:5,000) antibodies were purchased from Thermo Fisher Scientific, Inc. MYADM (cat. no. ABIN6059266; 1:5,000) and CLU (cat. no. ABIN6574258; the microtiter plate provided in this kit was pre-coated with antibodies specific to CLU, 1:50) antibodies were purchased from Antibodies-Online. Polystyrene ELISA plates (Nunc Maxisorp; Bion) were coated with capture antibodies (1:50) in bicarbonate buffer at 4°C overnight. After the coating solution was removed, the plates were washed three times with 200 μ l PBS containing 0.05% Tween-20 (PBST). The coated wells were then blocked for 1 h with 5% non-fat dry milk in PBST at room temperature. Equal amounts of samples were added to each well and the plates were incubated for 1 h at 37°C. The samples were then removed and the plates were washed three times with PBST. Horseradish peroxidase-conjugated antibodies (Thermo Fisher Scientific, Inc.; cat. nos. 32230 and 65-6120; dilutions, 1:5,000 and 1:3,000, respectively) in bicarbonate buffer were added and the plates were incubated at 37°C for 45 min. After washing with PBST, 3,3',5,5'-Tetramethylbenzidine substrate was added to each well, followed by incubation at 37°C for 15 min. The

reaction was stopped by adding 50 μ l 1 mol/l H_2SO_4 . The absorbance was read by an ELISA reader at 450 nm (with a reference wavelength of 620 nm). All samples were tested in duplicate.

Statistical analysis. Values are expressed as the mean \pm standard deviation. Multiple comparisons were performed using one-way ANOVA with Fisher's least-significant differences (LSD) test as the post-hoc test. $P < 0.05$ was considered to indicate a statistically significant difference. Genetic algorithm (GA), supervised neural networks (SNN) and quick classifier (QC) algorithms were applied to identify differentially expressed peptides distinguishing TBS after TB or TIT and ESLC.

Results

General information. Serum and BALF proteomic profiles of TBS after TB, TBS after TIT and ESLC groups were compared. There were no significant differences in age, BALF return rate, protein abundance (estimated by the rate of albumin in BALF/serum) between the three groups (Table SI). There were more female than male patients in the TB group (Table SI). Fr Fractionation of serum and BALF samples by MB-WCX and analysis by MALDI-TOF MS was performed to obtain the proteomic profiles of patients with TB (red), patients with TIT (green) and patients with ESLC (blue) with proteins ranging from 1,000 to 10,000 kDa (Fig. 1).

Table I. Mean levels of differentially expressed peptides in serum and BALF among the three groups.

A, Serum					
Mass (m/z)	P-value	Fisher's LSD ^a	TB	TIT	ESLC (mean)
1,532.24	0.011543	1-2; 1-3	15.63±8.97	6.68±2.90	8.14±2.98
6,816.51	0.019953	2-1	5.26±1.95	7.75±3.81	9.96±3.73
1,180.93	0.022359	1-3	14.01±8.00	6.80±2.90	9.47±2.80
4,185.05	0.030628	1-2	47.16±36.46	24.49±3.06	7.37±36.78
2,660.56	0.039298	2-1	30.28±27.30	47.49±41.55	72.25±26.88
6,844.58	0.040057	2-1; 2-3	9.85±5.58	10.26±9.35	15.18±5.65
4,419.72	0.042567	3-1	35.41±9.43	74.00±19.60	49.82±53.13
4,300.83	0.048204	3-1	35.85±15.15	58.70±10.47	53.15±21.94
B, BALF					
Mass (m/z)	P-value	Fisher's LSD ^a	TB	TIT	ESLC (mean)
6,029.68	0.015465	1-2; 1-3	81.86±51.11	47.49±19.69	29.78±52.77
4,200.65	0.015667	3-1; 3-2	11.41±10.66	32.95±3.89	6.15±31.95
4,186.06	0.019457	3-1; 3-2	20.21±20.95	56.60±7.86	10.66±55.13
6,701.81	0.026834	2-1; 2-3	17.96±11.32	11.61±28.48	31.22±5.37
7,929.01	0.030448	1-2; 1-3	607.65±529.57	205.62±454.00	226.75±214.01
5,763.15	0.032319	1-2	53.34±35.00	37.48±13.74	26.71±21.31
5,278.1	0.032377	1-2; 1-3	101.01±65.43	53.93±57.94	48.80±37.76
4,169.49	0.040676	3-1; 3-2	13.57±13.26	56.60±5.56	10.66±28.43
4,533.75	0.042205	1-3	11.78±6.37	5.76±4.34	7.03±3.05

^aComparisons: 1, TB; 2, ESLC; 3, TIT were statistically significant at a P<0.05. Data are presented as mean ± SD. BALF, bronchial alveolar lavage fluid; m/z, mass-to-charge ratio; LSD, least-significant differences test; TB, tuberculosis; TIT, tracheal intubation and tracheotomy; ESLC, early-stage lung cancer.

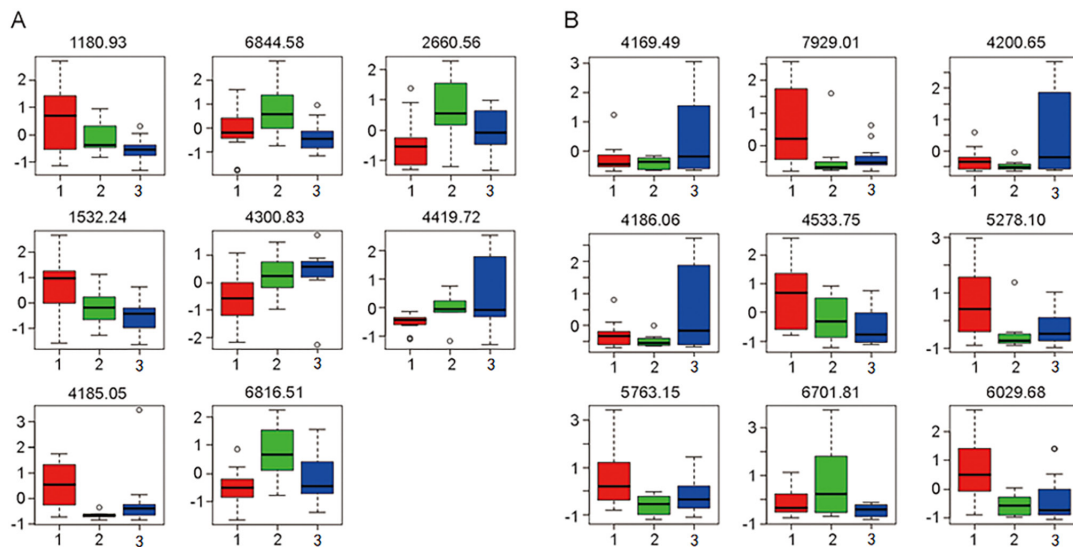


Figure 2. Box plots indicating the differences in peptide levels in (A) serum and (B) BALF among the different groups. A total of 8 peptides were identified to be differentially expressed in serum, including those with an m/z of 1,180.93 (myeloid-associated differentiation marker), 6,844.58 (undefined peptide), 2,660.56 (fibrinogen α -chain), 1,532.24 (clusterin), 4,300.83 (keratin, type I cytoskeletal 18), 4,419.72 (APOAI), 4,185.05 (AGT) and 6,816.51 (undefined peptide). Furthermore, 9 peptides were identified to be differentially expressed in BALF, including those with an m/z of 4,169.49 (APOAI), 7,929.01 (undefined peptide), 4,200.65 (argininosuccinatelyase), 4,186.06 (AGT), 4,533.75 (APOAI), 5,278.1 (undefined peptide), 5,763.15 (undefined peptide), 6,701.81 (undefined peptide), 6,029.68 (undefined peptide). Relative levels (fold change) of the proteins were presented in the box plots. Groups: 1 (red), tuberculosis; 2 (green), tracheal intubation and tracheotomy; and 3 (blue), early-stage lung cancer. BALF, bronchial alveolar lavage fluid; m/z, mass-to-charge ratio; APOAI, apolipoprotein A-I; ATG, angiotensinogen.

Table II. Peak selection of the algorithm models.

Algorithm	Serum peak selection (m/z)			BALF peak selection (m/z)		
	TB vs. TIT	TIT vs. ESLC	TB vs. ESLC	TB vs. TIT	TIT vs. ESLC	TB vs. ESLC
SNN	1531, 4420, 3859, 9010, 4435, 5544, 4153, 4185, 5506, 4644, 4467, 7481, 1312, 5716, 8618, 7356, 7029, 3588, 9539, 5753	1539	5266, 4300, 839, 4169	7769, 4170, 4534, 4136, 2022, 8621, 3276, 3086, 6960, 2423, 1722, 5279, 6831, 3475, 2711, 4941, 3905, 8323, 3012, 3463, 5218, 2316, 2090, 1427	5383	6030, 3463, 3905, 1942, 5384, 1743, 6811, 3012, 2316, 922, 5699, 7621, 5279, 7542
QC	855, 1050, 1066, 1150, 1180	839, 855, 861, 975, 1011, 1050, 1066, 1072, 1251, 1450, 1523, 1539, 2379, 2448, 2462, 2473	839, 2022, 2037, 2044, 2052, 2065, 2660, 2674, 3508, 3736, 4128, 4152, 4169, 4186, 4300, 7067, 9539	833, 1312, 1330, 1449, 2316, 3475, 4186, 4200, 4216, 4534, 5279, 7929, 8584, 8621	817, 833, 839, 845	6030
GA	1180, 3904, 3764, 2022, 4644	3314, 1251, 6888, 3486, 3401	3508, 1180, 7067, 4152, 4467	4186, 2723, 6029, 4941, 6960	6644, 4136, 839, 5383, 2032	5763, 2066, 2754, 3841, 5421

SNN, supervised neural network; QC, quick classifier; GA, genetic algorithm; BALF, bronchial alveolar lavage fluid; m/z, mass-to-charge ratio; TB, tuberculosis; TIT, tracheal intubation and tracheotomy; ESLC, early-stage lung cancer.

Differences in serum and BALF peptides. Using ClinProTools software to analyze serum samples, 155 peptide peaks were identified at an S/N threshold of 3 within the mass range analyzed (1,000-10,000 kDa). A fold change of >1.5 and $P < 0.05$ as determined by one-way ANOVA were set as the threshold for differentially expressed proteins and Fisher's LSD test was used to determine differences between pairs of groups. A total of 5 proteins, including CLU, AGT, FGA and two undefined peptides (Fisher's LSD 1-2 or 2-1) differed significantly between the TB and TIT groups and 5 of the peaks differed significantly between the TB and ESLC groups. Furthermore, one of the peaks differed significantly between the TIT and ESLC groups (Table IA). In BALF samples, using the same thresholds as above, 9 peptide peaks were identified. A total of 5 peptides were differentially expressed between the TB and TIT groups, 7 peptides differed between the TB and ESLC groups and 4 peaks differed significantly between the TIT and ESLC samples (Table IB).

Based on the macroscopic results of the multivariate statistical analysis, the tendency of the relative integrals of each metabolite to change in the three groups was further analyzed by box-and-whisker plots. These plots illustrated the progressive changes in metabolite levels in the TB group or TIT group relative to the ESLC group (Fig. 2).

Model building. The GA, SNN and QC model-building functions embedded in ClinPro Tools 2.2 software were used to establish a cross-validated classification model to distinguish TB, TIT and ESLC groups in terms of serum and BALF proteins. The peaks that were selected by these three algorithms are presented in Table II.

Identification of peptides by MALDI-TOF MS. To determine which peptides in the MS profiles are possible biomarkers, the current study attempted to identify those peptides with higher concentrations. The peptides in the Fisher model were purified and analyzed by MALDI-TOF MS and 6 serum peptides and 4 BALF peptides were successfully identified. A total of 8 peptides in serum, including MYADM (m/z 1,180.93), KRT18 (4,300.83), FGA (2,660.56), AGT (4,185.05), APOAI (4,419.72), CLU (1,532.24) and two undefined peptides (6,816.51 and 6,844.58) were successfully sequenced (Table III). In BALF samples, 9 peptides, including argininosuccinate lyase (ASL; 4,200.65), APOAI (two sequences: 4,169.49 and 4,533.75), AGT (4,186.06) and five undefined peptides (6,029.68, 5,763.15, 7,929.01, 6,701.81 and 5,278.1) were sequenced (Table III). AGT and APOAI simultaneously appeared in both serum and BALF samples. APOAI was identified in both serum and BALF samples by its sequence KAKPALEDLRQGLLPVLE SFKVSFLSALEEYTKKLNTQ, while AGT was confirmed as the sequence KPEVLEVTLNRPFLFAVY DQSATALHFLGRVANPLSTA. Compared with the TIT group, AGT and CLU were significantly upregulated and FGA was downregulated in serum from patients with TB, implying their potential roles in the pathogenesis of the disease.

Validation of differentially expressed peptides in serum by ELISA. To validate the results of MALDI-TOF MS, ELISA was applied for the quantification of the differentially expressed peptides in sera from 20 patients with TB, 20 patients with TIT and 20 patients with ESLC. Fold changes in the protein levels are presented in Fig. 3. The results indicated that MYADM, AGT and CLU were upregulated in the TB group as compared

Table III. List of detected sequences.

A, Serum			
Mass (M+H; kDa)	Protein symbol	Protein name	Sequence
1,180.93	MYADM	Myeloid-associated differentiation marker	M.PVTVTRTTITT.T
4,300.83	KRT18	Keratin, type I cytoskeletal 18	K.NREELDKYWSQQIEESTTVVTTQSAEVGAAETTLTEL.R
2,660.56	FGA	Isoform 1 of fibrinogen α -chain	A.DEAGSEADHEGTHSTKRGHAKSRPV.R
6,816.51	-	N/A	N/A
6,844.58	-	N/A	N/A
4,185.05	AGT	Angiotensinogen precursor	N.KPEVLEVTLNRPFLFAVYDQSATALHFLGRVANPLSTA.-
4,419.72	APOAI	Apolipoprotein A-I precursor	S.EKAKPALEDLRQGLLPVLESFKVSFLSALEEYTKKLNTQ.-
1,532.24	CLU	Clusterin precursor	R.RPHFFPKSRIV.R
B, BALF			
Mass (M+H; kDa)	Protein symbol	Protein name	Sequence
6,029.68	-	N/A	N/A
5,763.15	-	N/A	N/A
4,200.65	ASL	Argininosuccinatelyase	D.FVAEFLFWASLCM*THLSRM*AEDLILYCTKEFSFVQ.L
7,929.01	-	N/A	N/A
6,701.81	-	N/A	N/A
4,169.49	APOAI	Apolipoprotein A-I precursor	K.AKPALEDLRQGLLPVLESFKVSFLSALEEYTKKLNTQ.-
4,186.06	AGT	Angiotensinogen precursor	N.KPEVLEVTLNRPFLFAVYDQSATALHFLGRVANPLSTA.-
5,278.10	-	N/A	N/A
4,533.75	APOAI	Apolipoprotein A-I precursor	L.SEKAKPALEDLRQGLLPVLESFKVSFLSALEEYTKKLNTQ.-

M+H, protonated molecular ion; N/A, not available; BALF, bronchial alveolar lavage fluid.

with those in the TIT and ESLC groups, while KRT18, FGA and APOAI were downregulated in the TB group compared with those in the TIT and ESLC groups. Notably, patients with ESLC had relatively high serum FGA levels and low APOAI levels compared with those in the TIT group (Fig. 3). There was an indication that these proteins may serve as potential markers to distinguish patients with TBS after TB from patients with TBS due to other causes.

Discussion

Patients with tracheobronchial TB frequently encounter TBS, which may lead to pulmonary complications and death. In the clinic, prevention of TBS is critical to reduce the risk of death. Bronchoscopic or surgical interventions are used to restore airway patency once significant stenosis occurs (2). Although

certain studies focused on the biomarkers for pulmonary TB, the diagnosis of TBS after TB with non-invasive clinical tests appears to be particularly important (21,22). The present study aimed to identify putative biomarkers of TBS after tracheobronchial TB and the results revealed that MYADM, AGT, CLU and FGA in serum may serve as biomarkers for the diagnosis of TBS after tracheobronchial TB.

In the present study, MYADM was significantly upregulated in the serum of patients with TB compared with that in the ESLC group and downregulated in the serum of patients with TIT compared with that in the ESLC and TB groups. Full-length MYADM complementary (c)DNA was identified in a human bone marrow cDNA library in 2001 and was mapped to chromosome 19q 13.33-q 13.4 (23). MYADM is expressed in specialized domains on the membrane surface of human endothelial and epithelial cells and binds with actin (24).

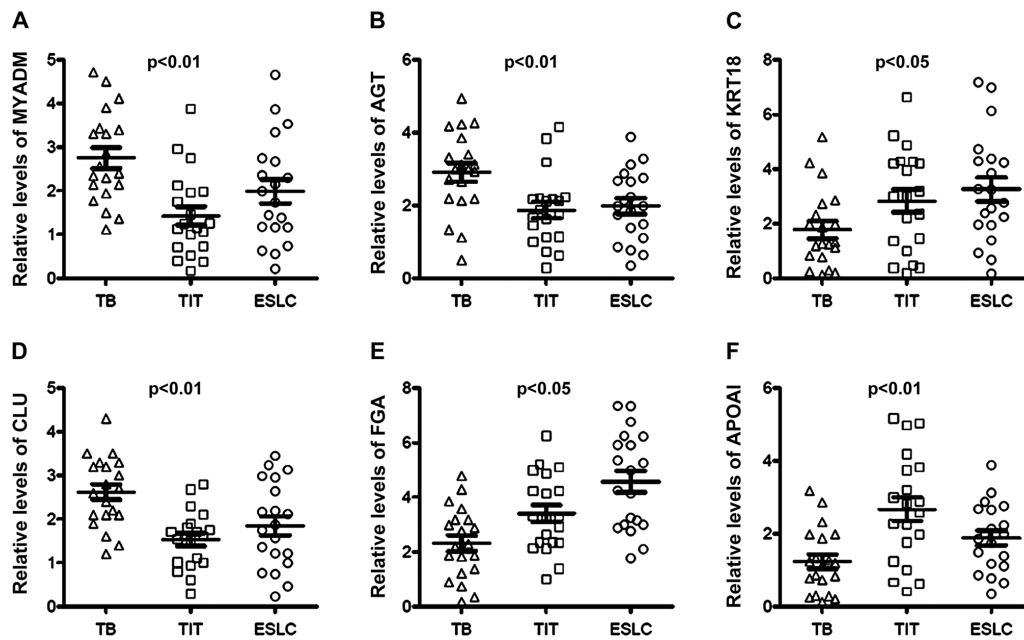


Figure 3. Fold changes of the protein levels in serum determined by ELISA. Serum (A) MYADM, (B) AGT, (C) KRT18, (D) CLU, (E) FGA and (F) APOAI were quantified using ELISA. MYADM, AGT and CLU levels were increased in TB patients compared with those in TIT and ESLC patients. On the contrary, KRT18, FGA and APOAI were distinctly decreased in TB patients compared with TIT and ESLC patients. TBS, tracheobronchial stenosis; TB, tuberculosis; ESLC, TIT, tracheal intubation and tracheotomy; early-stage lung cancer; MYADM, myeloid-associated differentiation marker; KRT18, keratin, type I cytoskeletal 18; FGA, fibrinogen α -chain; APOAI, apolipoprotein A-I; AGT, angiotensinogen; CLU, clusterin.

Additionally, MYADM colocalizes with Rac family small GTPase1 protein in membrane rafts during cell migration (25). Knockdown of MYADM with small interfering (si)RNA led to enhanced cell permeability, intercellular adhesion molecule-1 expression and leukocyte adhesion, which are characteristics of the inflammatory phenotype in endothelial cells (24). Notably, upregulation of MYADM specifically correlates with carotid neointimal formation, which promoted aortic artery smooth muscle cell (SMC) differentiation in a rat carotid artery balloon-injury model (26). Airway SMCs are recognized as a primary pathological determinant in lung diseases, including asthma and emphysema (27). Their dynamic and multifunctional behavior contributes to inflammation, fibroproliferation, abnormal wound healing, airway remodeling and hypertrophic scar formation and, therefore, narrowing of the airway lumen, leading to irreversible airway stenosis (28).

In the present study, FGA was downregulated in the serum of patients with TB compared with that in patients in the TIT and ESLC groups. Patients with aspirin-exacerbated respiratory disease, which is associated with asthma severity, have also been reported to exhibit reduced serum FGA levels (29).

The present results demonstrated that AGT levels were higher in sera in patients with TB compare to sera from patients in the TIT and ESLC groups; however, AGT levels in BALFs from patients with TB were lower compared with the BALFs from patients in the TIT group. AGT levels in BALFs were lower in patients with ESLC than in those with TB and TIT. AGT is thought to be involved in tumor angiogenesis and metastasis, as lung tumor growth and metastasis were attenuated in AGT (+/-) mice (30). The mechanisms of AGT-modulated airway stenosis require further elucidation.

The present results indicated that CLU was upregulated in the sera of patients with TB and it has been previously reported

to be differentially expressed in plasma from patients with active TB complicated with diabetes (31). Furthermore, CLU levels were decreased in BALF from patients with pulmonary fibrosis and facilitated epithelial cell regeneration during lung repair (32,33). CLU is a critical glycoprotein with key roles in homeostasis, inhibition of cell death and promotion of pro-survival signaling pathways (34). It is involved in several physiological and pathological states. Genetic variation of CLU is associated with Alzheimer's disease (AD) (35). Notably, CLU serves as a chaperon of amyloid β and has attracted considerable attention in the field of AD research (36). CLU was indicated to be elevated in several tumor types. CLU confers chemoresistance to numerous cancer types, including primary breast cancer (37), pancreatic cancer (38), lung cancer (39), osteosarcoma (40) and prostate cancer (41). Accordingly, custirsen, a second-generation antisense oligonucleotide, was designed to inhibit the expression of CLU.

In the present study, serum APOAI was indicated to be downregulated in patients with TB. This result is in concordance with those of previous studies. APOAI is the major protein component of high-density lipoprotein that has a key role in lipid metabolism and serves as a biomarker for cardiovascular diseases (42). Serum APOAI levels were negatively correlated with the onset of cerebral infarction in patients with carotid artery stenosis (43). Of note, a recent study demonstrated that APOAI, -AII and -AIV were decreased in patients with active TB (44). Furthermore, rifampicin treatment led to an increase in the level of APOAI in patients with TB; however, there was no statistical significance (45). Serum APOAI protein, quantified by isobaric tags for relative and absolute quantitation labeling coupled with two-dimensional liquid chromatography tandem MS, was markedly upregulated in patients cured of TB compared with that in untreated TB patients (46). APOAI is

expressed in the lung. Of note, APOAI^{-/-} mice presented with increased active lung inflammation and airway hyperresponsiveness (47). APOAI mimetics reduced the responses in the mouse model of asthma (48). Further studies are required to explore the putative implications of APOAI in the pathology and treatment of the disease.

The epithelial-mesenchymal transition is recognized as a key process in the initiation of cancer and it is accompanied by downregulation of KRT8/KRT18, which was indicated to be barely expressed in two intestinal cell lines, murine CT26 and rat IEC-6 cells (49). In IEC-6 cells, the KRT18 promoter was determined to be hypermethylated and in CT26 cells, a 9-amino acid in-frame insertion in the gene was identified. Matrigel assays indicated that restoration of KRT18 reduced CT26 cell invasion (49). The results demonstrated that the restoration of KRT18 reduced E-cadherin expression in IEC-6 cells; however, reduced expression was not observed in CT26 cells. Furthermore, KRT18 expression was modulated by early growth response 1 (EGR1) in non-small-cell lung carcinoma. Robust EGR1 expression and regulation of KRT18 led to reduced cell mobility and migration, and activated tumor cell apoptosis (50). Additionally, KRT18 was indicated to be associated with cancer cell metastasis. siRNA-mediated knockdown of KRT18 increased the migration and invasion of HepG2 and Eca109 cells (51). However, the roles and mechanisms of KRT18 in TB and tracheobronchial TB-induced TBS remain to be elucidated.

In conclusion, in the present study, MALDI-TOF MS was used to analyze proteins in the serum and BALF from patients with TB, ESLC and TIT to identify potential biomarkers for TBS secondary to tracheobronchial TB. Several candidate proteins, including MYADM, APOAI and KRT18, should be further examined for their roles in the pathophysiology of TBS. These proteins are involved in cell migration, permeability, adhesion, invasion, differentiation, neointima formation and tumor metastasis, which indicates a combination of pathological changes during TBS. These candidate proteins may be promising diagnostic tools and therapeutic targets and provide additional insight into the mechanisms underlying TBS after tracheobronchial TB.

Acknowledgements

Not applicable.

Funding

The current work was supported by the Capital Health Development Research Project (grant no. 2016-2-2048).

Availability of data and materials

The datasets used and/or analyzed during the current study are available from the corresponding author on reasonable request.

Authors' contributions

BP, XQ and JZ conceptualized and designed the current study and acquired, analyzed and interpreted data. ZD analyzed and interpreted data. BP and JZ drafted the manuscript. JZ criti-

cally revised the manuscript for important intellectual content. YP and TW acquired data. All authors read and approved the final manuscript.

Ethics approval and consent to participate

All of the patients provided written informed consent to participate in the current study and for use of their medical data according to the provisions of the Declaration of Helsinki. The protocol of the current study was approved by the Institutional Ethics Committee of Beijing Tian Tan Hospital, Capital Medical University (Beijing, China).

Patient consent for publication

Not applicable.

Competing interests

The authors declare that they have no competing interests.

References

- Hirshoren N and Eliashar R: Wound-healing modulation in upper airway stenosis-Myths and facts. *Head Neck* 31: 111-126, 2009.
- Siow WT and Lee P: Tracheobronchial tuberculosis: A clinical review. *J Thorac Dis* 9: E71-E77, 2017.
- Nemati A, Safavi E, GhasemiEsfe M, Anaraki MZ, Firoozbakhsh S, Khalilzadeh O and Anvari M: Fistula formation between the right and left main bronchus caused by endobronchial tuberculosis. *Am J Med Sci* 343: 330-331, 2012.
- Kashyap S, Mohapatra PR and Saini V: Endobronchial tuberculosis. *Indian J Chest Dis Allied Sci* 45: 247-256, 2003.
- Um SW, Yoon YS, Lee SM, Yim JJ, Yoo CG, Chung HS, Kim YW, Han SK, Shim YS and Kim DK: Predictors of persistent airway stenosis in patients with endobronchial tuberculosis. *Int J Tuberc Lung Dis* 12: 57-62, 2008.
- Shahzad T and Irfan M: Endobronchial tuberculosis-a review. *J Thorac Dis* 8: 3797-3802, 2016.
- Mondoni M, Repossi A, Carlucci P, Centanni S and Sotgiu G: Bronchoscopic techniques in the management of patients with tuberculosis. *Int J Infect Dis* 64: 27-37, 2017.
- Pathak V, Shepherd RW and Shojae S: Tracheobronchial tuberculosis. *J Thorac Dis* 8: 3818-3825, 2016.
- England K, Masini T and Fajardo E: Detecting tuberculosis: Rapid tools but slow progress. *Public Health Action* 9: 80-83, 2019.
- Fan NJ, Gao CF and Wang XL: Tubulin beta chain, filamin A alpha isoform 1, and cytochrome b-c1 complex subunit 1 as serological diagnostic biomarkers of esophageal squamous cell carcinoma: A proteomics study. *OMICS* 17: 215-223, 2013.
- Sobsey CA, Ibrahim S, Richard VR, Gaspar V, Mitsa G, Lacasse V, Zahedi RP, Batist G and Borchers CH: Targeted and untargeted proteomics approaches in biomarker development. *Proteomics* 20: e1900029, 2020.
- Venkatesh A, Gil C, Fuentes M, LaBaer J and Srivastava S: A Perspective on Proteomics of Infectious Diseases. *Proteomics Clin Appl* 12: e1700139, 2018.
- Dong W, Qiu C, Gong D, Jiang X, Liu W, Liu W, Zhang L and Zhang W: Proteomics and bioinformatics approaches for the identification of plasma biomarkers to detect Parkinson's disease. *Exp Ther Med* 18: 2833-2842, 2019.
- Beavis RC and Chait BT: Rapid, sensitive analysis of protein mixtures by mass spectrometry. *Proc Natl Acad Sci USA* 87: 6873-6877, 1990.
- Stoeckli M, Farmer TB and Caprioli RM: Automated mass spectrometry imaging with a matrix-assisted laser desorption/ionization time-of-flight instrument. *J Am Soc Mass Spectrom* 10: 67-71, 1999.
- Peng Y, Zhang Q, Xu C and Shi W: MALDI-TOF MS for the rapid identification and drug susceptibility testing of filamentous fungi. *Exp Ther Med* 18: 4865-4873, 2019.

17. Cho YT, Su H, Wu WJ, Wu DC, Hou MF, Kuo CH and Shiea J: Biomarker Characterization by MALDI-TOF/MS. *Adv Clin Chem* 69: 209-254, 2015.
18. Davies HA: The ProteinChip System from Ciphergen: A new technique for rapid, micro-scale protein biology. *J Mol Med (Berl)* 78: B29, 2000.
19. Deng BG, Yao JH, Liu QY, Feng XJ, Liu D, Zhao L, Tu B and Yang F: Comparative serum proteomic analysis of serum diagnosis proteins of colorectal cancer based on magnetic bead separation and maldi-tof mass spectrometry. *Asian Pac J Cancer Prev* 14: 6069-6075, 2013.
20. Malys BJ, Piotrowski ML and Owens KG: Diagnosing and correcting mass accuracy and signal intensity error due to initial ion position variations in a MALDI TOFMS. *J Am Soc Mass Spectrom* 29: 422-434, 2018.
21. Cho Y, Park Y, Sim B, Kim J, Lee H, Cho SN, Kang YA and Lee SG: Identification of serum biomarkers for active pulmonary tuberculosis using a targeted metabolomics approach. *Sci Rep* 10: 3825, 2020.
22. Isa F, Collins S, Lee MH, Decome D, Dorvil N, Joseph P, Smith L, Salerno S, Wells MT, Fischer S, *et al*: Mass spectrometric identification of urinary biomarkers of pulmonary tuberculosis. *EBioMedicine* 31: 157-165, 2018.
23. Cui W, Yu L, He H, Chu Y, Gao J, Wan B, Tang L and Zhao S: Cloning of human myeloid-associated differentiation marker (MYADM) gene whose expression was up-regulated in NB4 cells induced by all-trans retinoic acid. *Mol Biol Rep* 28: 123-138, 2001.
24. Aranda JF, Reglero-Real N, Marcos-Ramiro B, Ruiz-Sáenz A, Fernández-Martín L, Bernabé-Rubio M, Kremer L, Ridley AJ, Correas I, Alonso MA, *et al*: MYADM controls endothelial barrier function through ERM-dependent regulation of ICAM-1 expression. *Mol Biol Cell* 24: 483-494, 2013.
25. Aranda JF, Reglero-Real N, Kremer L, Marcos-Ramiro B, Ruiz-Sáenz A, Calvo M, Enrich C, Correas I, Millán J and Alonso MA: MYADM regulates Rac1 targeting to ordered membranes required for cell spreading and migration. *Mol Biol Cell* 22: 1252-1262, 2011.
26. Sun L, Bai Y, Zhao R, Sun T, Cao R, Wang F, He G, Zhang W, Chen Y, Ye P, *et al*: Oncological miR-182-3p, a novel smooth muscle cell phenotype modulator, evidences from model rats and patients. *Arterioscler Thromb Vasc Biol* 36: 1386-1397, 2016.
27. Panettieri RA Jr: Airway smooth muscle: An immunomodulatory cell. *J Allergy Clin Immunol* 110 (Suppl): S269-S274, 2002.
28. Ozier A, Allard B, Bara I, Girodet PO, Triantafyllidis T, Marthan R and Berger P: The pivotal role of airway smooth muscle in asthma pathophysiology. *J Allergy (Cairo)* 2011: 742710, 2011.
29. Kim HJ, Park JS, Heo JS, Moon KY and Park CS: Plasma apolipoprotein H levels are different between aspirin induced respiratory diseases and aspirin tolerant asthma. *Pulm Pharmacol Ther* 27: 184-189, 2014.
30. Choi JH, Nguyen MP, Lee D, Oh GT and Lee YM: Hypoxia-induced endothelial progenitor cell function is blunted in angiotensinogen knockout mice. *Mol Cells* 37: 487-496, 2014.
31. Zhang X, Ma A, Sun S and Sun Y: Proteomic analysis of plasma in adult active pulmonary tuberculosis patients with diabetes mellitus. *Clin Lab* 61: 1481-1490, 2015.
32. Peix L, Evans IC, Pearce DR, Simpson JK, Maher TM and McAnulty RJ: Diverse functions of clusterin promote and protect against the development of pulmonary fibrosis. *Sci Rep* 8: 1906, 2018.
33. Habel DM, Camelo A, Espindola M, Burwell T, Hanna R, Miranda E, Carruthers A, Bell M, Coelho AL, Liu H, *et al*: Divergent roles for clusterin in lung injury and repair. *Sci Rep* 7: 15444, 2017.
34. Wilson MR and Zoubeidi A: Clusterin as a therapeutic target. *Expert Opin Ther Targets* 21: 201-213, 2017.
35. Nordestgaard LT, Tybjaerg-Hansen A, Rasmussen KL, Nordestgaard BG and Frikke-Schmidt R: Genetic variation in clusterin and risk of dementia and ischemic vascular disease in the general population: Cohort studies and meta-analyses of 362,338 individuals. *BMC Med* 16: 39, 2018.
36. Foster EM, Dangla-Valls A, Lovestone S, Ribe EM and Buckley NJ: Clusterin in Alzheimer's Disease: Mechanisms, genetics, and lessons from other pathologies. *Front Neurosci* 13: 164, 2019.
37. Wang Y, Wang X, Zhao H, Liang B and Du Q: Clusterin confers resistance to TNF-alpha-induced apoptosis in breast cancer cells through NF-kappaB activation and Bcl-2 overexpression. *J Chemother* 24: 348-357, 2012.
38. Tang Y, Liu F, Zheng C, Sun S and Jiang Y: Knockdown of clusterin sensitizes pancreatic cancer cells to gemcitabine chemotherapy by ERK1/2 inactivation. *J Exp Clin Cancer Res* 31: 73, 2012.
39. Panico F, Rizzi F, Fabbri LM, Bettuzzi S and Luppi F: Clusterin (CLU) and lung cancer. *Adv Cancer Res* 105: 63-76, 2009.
40. Ma J, Gao W and Gao J: sCLU as prognostic biomarker and therapeutic target in osteosarcoma. *Bioengineered* 10: 229-239, 2019.
41. Bertacchini J, Mediani L, Beretti F, Guida M, Ghalali A, Brugnoli F, Bertagnolo V, Petricoin E, Poti F, Arioli J, *et al*: Clusterin enhances AKT2-mediated motility of normal and cancer prostate cells through a PTEN and PHLPP1 circuit. *J Cell Physiol* 234: 11188-11199, 2019.
42. Charlton-Menys V and Durrington P: Apolipoproteins AI and B as therapeutic targets. *J Intern Med* 259: 462-472, 2006.
43. Dong Z, Guo Q, Sun L, Li F, Zhao A, Liu J, Qu P, Zhu Q, Xiao C, Niu F, *et al*: Serum lipoprotein and RBC rigidity index to predict cerebral infarction in patients with carotid artery stenosis. *J Clin Lab Anal* 32: e22356, 2018.
44. Mateos J, Estévez O, González-Fernández Á, Anibarro L, Pallarés A, Reljic R, Mussá T, Gomes-Mauêia C, Nguilichane A, Gallardo JM, *et al*: Serum proteomics of active tuberculosis patients and contacts reveals unique processes activated during *Mycobacterium tuberculosis* infection. *Sci Rep* 10: 3844, 2020.
45. Albanna AS, Bachmann K, White D, Valiquette C and Menzies D: Serum lipids as biomarkers for therapeutic monitoring of latent tuberculosis infection. *Eur Respir J* 42: 547-550, 2013.
46. Wang C, Wei LL, Shi LY, Pan ZF, Yu XM, Li TY, Liu CM, Ping ZP, Jiang TT, Chen ZL, *et al*: Screening and identification of five serum proteins as novel potential biomarkers for cured pulmonary tuberculosis. *Sci Rep* 5: 15615, 2015.
47. Wang W, Xu H, Shi Y, Nandedkar S, Zhang H, Gao H, Feroah T, Weihrauch D, Schulte ML, Jones DW, *et al*: Genetic deletion of apolipoprotein A-I increases airway hyperresponsiveness, inflammation, and collagen deposition in the lung. *J Lipid Res* 51: 2560-2570, 2010.
48. Yao X, Dai C, Fredriksson K, Dagur PK, McCoy JP, Qu X, Yu ZX, Keeran KJ, Zywicke GJ, Amar MJ, *et al*: 5A, an apolipoprotein A-I mimetic peptide, attenuates the induction of house dust mite-induced asthma. *J Immunol* 186: 576-583, 2011.
49. Kwan R, Looi KS and Omary MB: Absence of keratins 8 and 18 in rodent epithelial cell lines associates with keratin gene mutation and DNA methylation: Cell line selective effects on cell invasion. *Exp Cell Res* 335: 12-22, 2015.
50. Zhang H, Chen X, Wang J, Guang W, Han W, Zhang H, Tan X and Gu Y: EGR1 decreases the malignancy of human non-small cell lung carcinoma by regulating KRT18 expression. *Sci Rep* 4: 5416, 2014.
51. Wang X, Lao Y, Xu N, Xi Z, Wu M, Wang H, Li X, Tan H, Sun M and Xu H: Oblongifolin C inhibits metastasis by up-regulating keratin 18 and tubulins. *SciRep* 5: 10293, 2015.



This work is licensed under a Creative Commons Attribution-NonCommercial-NoDerivatives 4.0 International (CC BY-NC-ND 4.0) License.